Novel Protein Crystal Growth Electrochemical Cell For Applications In X-ray Diffraction and Atomic Force Microscopy

ARTICLE *in* CRYSTAL GROWTH & DESIGN · JULY 2011

Impact Factor: 4.89 · DOI: 10.1021/cg200485v

8 AUTHORS, INCLUDING:

Adela Rodríguez-Romero
Universidad Nacional Autónoma de México
66 PUBLICATIONS **875** CITATIONS
SEE PROFILE

Enrique Rudiño-Piñera
Universidad Nacional Autónoma de México
44 PUBLICATIONS **305** CITATIONS
SEE PROFILE

Vivian Stojanoff
Brookhaven National Laboratory
131 PUBLICATIONS **1,484** CITATIONS
SEE PROFILE

Abel Moreno
Universidad Nacional Autónoma de México
81 PUBLICATIONS **969** CITATIONS
SEE PROFILE

CRYSTAL GROWTH & DESIGN

ARTICLE

pubs.acs.org/crystal

Novel Protein Crystal Growth Electrochemical Cell For Applications In X-ray Diffraction and Atomic Force Microscopy

Gabriela Gil-Alvaradejo,[†] Rayana R. Ruiz-Arellano,[†] Christopher Owen,[‡] Adela Rodríguez-Romero,[†] Enrique Rudiño-Piñera,[§] Moriamou K. Antwi,[⊥] Vivian Stojanoff,[‡] and Abel Moreno*[,†]

[†]Instituto de Química, Universidad Nacional Autónoma de México, México, D.F. 04510 Mexico

[‡]Brookhaven National Laboratory, National Synchrotron Light Source Bldg 725D, Upton New York 11873, United States

[§]Departamento de Medicina Molecular y Bioprocesos, Instituto de Biotecnología, Universidad Nacional Autónoma de México, Av. Universidad 2001, Cuernavaca, Morelos, 62210, Mexico

[⊥]St. Joseph's College, 245 Clinton Avenue Brooklyn, New York 11205, United States

Supporting Information

ABSTRACT: A new crystal growth cell based on transparent indium tin oxide (ITO) glass-electrodes for electrochemically assisted protein crystallization allows for reduced nucleation and crystal quality enhancement. The crystallization behavior of lysozyme and ferritin was monitored as a function of the electric current applied to the growth cell. The X-ray diffraction analysis showed that for specific currents, the crystal quality is substantially improved. No conformational changes were observed in the 3D crystallographic structures determined for crystals grown under different electric current regimes. Finally, the strong crystal adhesion on the surface of ITO electrode because of the electroadhesion allows a sufficiently strong fixing of the protein crystals, to undergo atomic force microscopy investigations in a fluid cell.

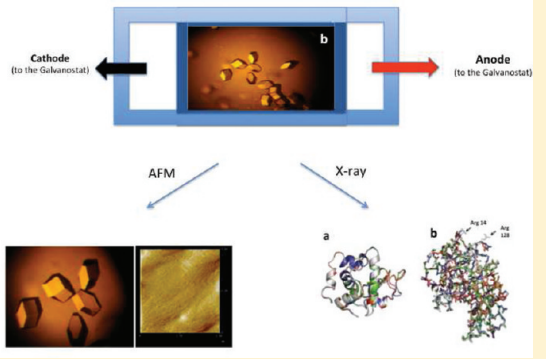

1. INTRODUCTION

Since Chin et al., pioneering work on the electrochemically assisted process of estradiol 17β-dehydrogenase, the idea of protein molecules behaving as macroions fell into a long lethargy.[1] In the late 1990s, two contributions[2,3] revived this research with theoretical and experimental results on the response of chromoproteins subjected to external pressure and electric fields. Thereafter new studies performed by Aubry and co-workers,[4,5] as well as Nanev and Penkova[6] applying external electric fields to the protein crystallization solution, showed that it is possible to reduce lysozyme nucleation, and to control the kinetics of the crystallization process. The use of internal electric fields merging capillary tubes and gels was first proposed by Mirkin et al., (2003).[7] A new concept was introduced by Moreno and Rivera in 2005[8] who used highly oriented pyrolytic graphite electrodes to crystallize ferritin. The use of different electrodes and configurations has been subject of three recent reviews.[9−11]

Obtaining high quality protein single crystals of a size large enough for X-ray analysis remains a bottleneck in structural biology research. Since the beginning of the 1990s, novel and miniaturized methods are being developed to obtain crystals in smaller droplets and in a shorter time.[12] Additional efforts are being made to optimize the X-ray data collection and the data processing methods, using powerful personal computers. However, there are only few results focused on the understanding of the crystallization process based on physicochemical approaches that use physical parameters to improve the crystal quality. Some contributions on the crystal growth process of different proteins grown under the influence of electric fields, voltage pulses (at controlled potentials and currents) that use different configurations, have been recently published.[13,14] There are some approaches already published combining electric and magnetic fields,[15] gels and magnetic fields,[16,17] or only magnetic fields in solution to control the orientation and crystal quality on proteins.[18−20]

Here we present a new crystal growth cell with parallel indium tin oxide (ITO) electrodes. The nucleation and crystal growth behavior of lysozyme and ferritin in the presence of different electric currents was monitored at constant temperature. Crystal quality was determined by X-ray crystallography and crystal surface analysis by atomic force microscopy (AFM). We found that for each protein crystals grown under specific current values showed better quality when tested by X-ray diffraction. No conformational changes were found in the 3D crystallographic structures because of the electroadhesion process.

2. EXPERIMENTAL SECTION

The crystal growth cell consisted of two polished float conductive ITO (indium tin oxide electrodes) glasses of 2.5 × 1.5 cm^2, with a resistance ranging from 4 to 8 Ohms (Delta Technologies, Minnesota U.S.A.), as shown in Figure 1. The two electrodes (ITO glasses) were

Received: April 15, 2011
Revised: June 27, 2011
Published: July 12, 2011

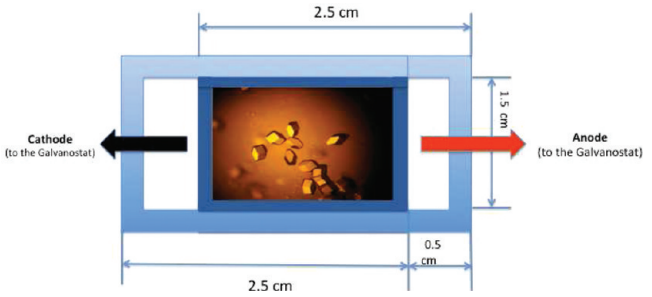

Figure 1. Growth cell and experimental set up using ITO transparent electrodes.

Table 1. Optimal Batch Crystallization Conditions for Lysozyme and Ferritin

protein	optimal batch crystallization conditions (stock solutions)	final proportion	optimal current applied
lysozyme		1:1	6 μA
	• protein concentration 80 mg/mL		
	• NaCl 80 mg/mL [Buffer acetate pH 4.45 (100 mM)]		
ferritin		1:1:1	2 μ to 6 μA
	• protein concentration 23 mg/mL		
	• $[CdSO_4]/[(NH_4)_2SO_4]$ = 0.08M/1M		
	• H_2O [buffer citrate pH 5.52 (100 mM)]		

placed parallel to each other. The cell was closed using a "U-like" elastic latex material, sealed with silicon after closing the growth cell. The conductive ITO coated surfaces were placed inward, facing each other. Each of the ITO electrodes was displaced by 0.5 cm relative to each other to provide the appropriate connection area with the electric alligators between the Galvanostat (VIMAR FCC-17) and the electrodes. Each cell had a volume capacity of approximately 100 μL. The growth cell was filled with protein and precipitating agent. The batch crystallization conditions for each protein are shown in Table 1. After closing the cell, the system was connected to the Galvanostat that supplied a direct current, but not alternating one.

During the nucleation and crystallization process the cells were hold at constant temperature. The proteins used for these experiments were Ferritin from horse spleen (Sigma, code F4503), and Hen Egg White Lysozyme (Seikagaku Corp., code 100940). All chemicals were analytical degree Fluka.

For each protein in duplicate experiments, four cells were set up using a constant current along the crystallization process (which usually takes place in 48 h): 2, 4, 6, and 8 μA, on a Galvanostat while maintaining a constant T = 18 °C. The temperature (with an accuracy ±0.5 °C) was fixed by means of a temperature controlled cabinet (T-Incubator GE model Profile). The galvanostat was programed for applying a direct current at fixed values (2, 4, 6, or 8 μA according to the experiment). The electric potential difference (voltage), which is usually called the electric tension was compensated by the galvanostat varying the potential difference to keep constant the direct current applied to the growth cell along the experiment. It is worth mentioning that in all cases there was no any electrochemical reaction (not redox reaction) between protein and electrodes tested by cyclic voltammetry using the electrochemical modulus of the atomic force microscope (EC-AFM Nanoscope IIIa Veeco Co). To recover the crystals (after 48 h), the silicon must be melted using an electric heating gun. This will create a gap to facilitate crystal extraction for further studies.

For atomic force microscopy, a Nanoscope IIIa (Veeco Co.) was used in contact mode using a fluid cell. All experiments were performed at the solid/liquid interface at room temperature. For this study, one of the ITO electrodes containing the electrodeposited protein crystals was used as a sample holder; being perfectly cut to be adapted to the AFM head and fluid cell for scanning. All images were taken in the contact mode with low scanning forces of 0.3 N/m to avoid surface damage. Scan speed was typically 1.97 Hz. Optical images were taken in situ using a Zeiss StemiSV11 stereoscopic microscope and digital camera coupled to the AFM.

The lysozyme crystals were retrieved and analyzed by X-ray diffraction using a Rigaku/MSC Micromax-007 X-ray generator (copper anode) with an Raxis-IV^{++} detector. For ferritin crystals, due to the size of the crystals, synchrotron radiation was necessary. Crystals were grown in situ ready for X-ray analysis under specific current regimes. The cubic-octahedral planar-shaped of ferritin faces, were perpendicular to the ITO electrodes allowing them to be scanned by AFM.

For synchrotron radiation, X-ray data up to 2.4 Å resolution were collected on the X6A beamline at the National Synchrotron Light Source, Brookhaven National Laboratory, Upton, NY. Several data sets of 20, 45, and 180 oscillation images (1 degree) were collected with an ADSC Quantum Detector 270. The X-ray data were integrated and scaled with the HKL 2000 package.[21]

3. RESULTS AND DISCUSSION

For the particular case of lysozyme the following behavior was observed: crystals obtained at 4 μA and 8 μA were less in number compare to the better and bigger crystals obtained at 6 μA. However, for these two current values, all crystals showed defects on the surface faces that were not observed for crystals grown at 6 μA. The crystals obtained at current values of 8 μA and higher showed a black shadow on their surface. The higher the current, 8 μA and up, the higher desorption of Indium and Tin from ITO electrodes causing a brown precipitation around protein crystals (at this point, anomalous voltage values were observed). This behavior did not happen at lower current values between 2 μA and 6 μA (Figure 2a−d). On the other hand, when all crystals were analyzed by X-ray diffraction, there seemed to be a specific current that produced crystals showing better quality. The lysozyme crystals obtained at current of 2 μA were analyzed by X-ray diffraction, and were slightly better but not significaly much better than the control. The best lysozyme crystals consistently showed lower mosaicity values, higher $I/\sigma(I)$ signal, and better resolution values. On the basis of these analyses, the best crystals are those grown at 6 μA (see Table 2). In terms of crystal habit these crystals were perfectly well shaped without any visible defects.

To better assess the quality of lysozyme crystals grown in the presence of electrical fields, the 3D molecule structure was compared to that of the control crystals (Figure 3). The comparison showed no substantial changes, except for Arginines14 and 128. However, high-quality electron density maps were obtained for the best crystals grown at 6 μA. Figure 3 shows the backbone ribbon representation of the 3D X-ray structures of: (a) lysozyme control crystal (gray color) showing the overlapping with lysozyme 4 μA (red), 6 μA (green), and 8 μA (blue); (b) C_α representation of lysozyme at the same conditions as shown for (a). Only a slightly variation is observed in the conformational state of Arginines 14 and 128, but this is not a significant crystallographic difference. For instance, the r_{msd} for lysozyme crystals grown at 4 μA and 6 μA was estimated to be 0.13 Å, for crystals grown at

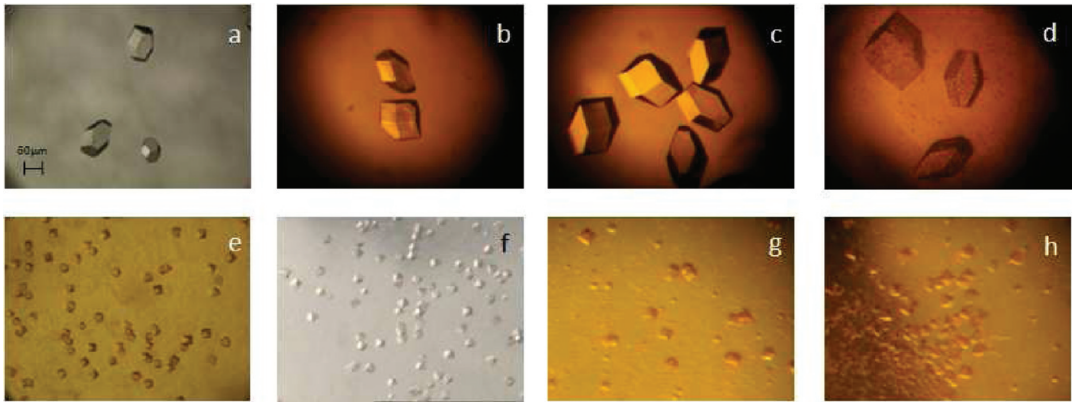

Figure 2. Crystal growth behavior applying different current values to the crystal growth cell: (a−d) for lysozyme and (e−h) for ferritin. Applied current to the cell: (a) lysozyme control, (b) 4 μA, (c) 6 μA, and (d) 8 μA, (e) ferritin control, (f) 2 μA, (g) 4 μA, and (h) 6 μA. The scale bar of 50 μm is the same for all pictures (a−h).

Table 2. Summary of Data Collection Statistics for Hen Egg White Lysozyme Crystals, Control and Grown in Electric Field

	control crystal 1	control crystal 2	4 μA crystal 1	4 μA crystal 2	6 μA crystal 1	6 μA crystal 2	8 μA crystal 1	8 μA crystal 2
space group	$P4_32_12$	$P4_32_12$	$P4_32_12$	$P4_32_12$	$P4_32_12$	$P4_32_12$	$P4_32_12$	$P4_32_12$
unit cell dimensions *a*, *b*, *c*	77.10 77.10	77.09 77.09	77.22 77.22	77.07 77.07	78.92 78.92	76.78 76.78	78.72 78.72	78.37 78.37
$\alpha = \beta = \gamma$	37.03	37.03	36.92	36.96	36.88	36.94	37.05	36.93
	90.00	90.00	90.00	90.00	90.00	90.00	90.00	90.00
mosaicity	1.81	1.76	2.63	4.16	2.46	1.80	0.40	2.62
resolution range	34.48−1.80 (1.86−1.80)	34.48−1.90 (1.97−1.90)	38.61−2.85 (2.95−2.85)	38.53−1.90 (1.97−1.90)	39.46−1.70 (1.76−1.70)	38.39−1.70 (1.76−1.70)	39.36−2.00 (2.07−2.00)	33.41−1.90 (1.97−1.90)
total number of reflections	69 108	58 881	19 703	41 517	65 032	84 016	42 896	55 183
number of unique reflections	10 723	9186	2845	8770	13 284	12 520	8262	9479
average redundancy	6.44 (6.66)	6.41 (6.61)	6.93 (7.25)	4.73 (4.88)	4.90 (5.30)	6.71 (6.78)	5.19 (5.02)	5.82 (5.63)
% Completeness	99.1 (98.7)	99.4 (99.2)	99.8 (100.0)	95.1 (96.9)	99.7 (100.0)	99.0 (99.3)	99.5 (99.8)	99.5 (99.9)
R_{merge}	0.085 (0.464)	0.086 (0.393)	0.182 (0.485)	0.057 (0.444)	0.054 (0.441)	0.047 (0.298)	0.037 (0.342	0.078 (0.500)
R_{meas}	0.092 (0.503)	0.093 (0.425)	0.197 (0.523)	0.063 (0.491)	0.061 (0.487)	0.050 (0.322)	0.351 (0.382)	0.085 (0.552)
R_{measA} (*I*+,*I*− reflns kept apart)	0.091 (0.500)	0.091 (0.421)	0.195 (0.528)	0.063 (0.490)	0.057 (0.432)	0.050 (0.322)	0.378 (0.384)	0.084 (0.547)
reduced χ^2	0.95 (0.83)	0.90 (0.81)	0.96 (0.89)	0.99 (0.87)	0.92 (0.82)	0.98 (1.14)	1.12 (1.50)	0.95 (0.85)
$\langle I/\sigma(I)\rangle$	9.2 (2.4)	9.7 (2.9)	6.1 (2.6)	12.7 (2.0)	11.1 (2.2)	17.3 (4.8)	10.8 (6.3)	9.2 (2.2)

6 μA and 8 μA it was 0.20 Å and finally for crystals grown at 8 μA and 4 μA it was 0.16 Å. From the crystallographic point of view, taking into account these r_{msd} values it is possible to conclude that there are no substantial changes in the 3D structure.

Ferritin crystals were grown for 30 h in situ (in the conditions shown in Table 1), before being analyzed in synchrotron radiation. In this case, control crystals and crystals grown at 2 μA, 4 μA, and 6 μA (Figure 2e−h) were analyzed in duplicate using the maximum of completeness in the data collection to guarantee proper X-ray diffraction. Table 3 shows statistics obtained from the X-ray diffraction analysis for ferritin crystals. Although high quality single crystals were obtained in the control setting, the best crystals grew when applying currents between 2 and 6 μA as shown in Table 3. It is worth mentioning that for ferritin we did not observe any changes in 3D crystal structures; they were exactly the same. This trend might be due to ferritin's cubic space group ($F432$), which is isotropic. The presence of iron in the internal core of this protein probably helped to compress the crystal packing when applying the direct electric current. For future investigations different space groups (polar and nonpolar) and different crystallographic systems, as well as, redox and nonredox proteins will be explored.

To understand the mechanism of protein nucleation and crystal growth inside of our crystal growth cell containing ITO transparent electrodes, it is necessary to consider the existence of an electric double layer formed along the electrode when applying a direct current. From the electrochemical point of view, it is well-known that when an electrode is dipped into an electrolyte solution, an electric double layer is formed around the electrode owing to the asymmetric forces felt by the electrolytes. This double layer is composed of an initial plane of water molecules with their dipoles oriented with respect to the electrode charge

dx.doi.org/10.1021/cg200485v |*Cryst. Growth Des.* 2011, 11, 3917–3922

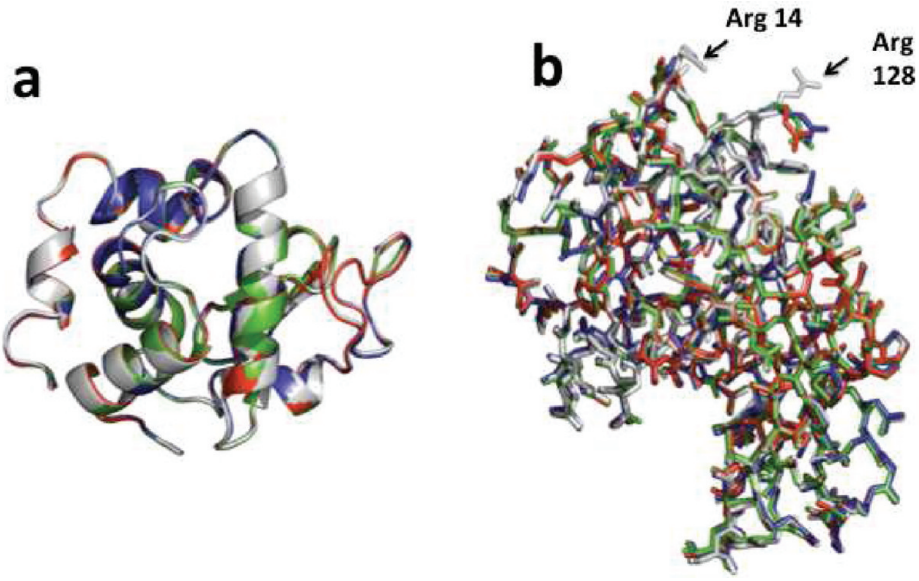

Figure 3. Ribbon representation of the 3D X-ray structure models of hen egg white lysozyme. (a) control (gray), 4 μA (red), 6 μA (green) and 8 μA (blue); (b) C_α representation of the control crystal compared with the same structures shown in a.

Table 3. Summary of Data Collection Statistics for Horse Spleen Ferritin Crystals, Control and Grown in Electric Field

	control	2 μA	4 μA	6 μA
space group	*F*432	*F*432	*F*432	*F*432
unit cell dimensions	181.77	181.84	182.38	182.00
mosaicity	0.530	0.308	0.675	0.308
resolution range	25.00−2.27 (2.31−2.27)	25.00−1.97 (2.00−1.97)	25.00−2.24 (2.28−2.24)	25.00−2.07 (2.11−2.07)
total number of reflections	2 804 198	1 189 907	720 448	2 228 266
number of unique reflections	12400	18 819	13 091	16 282
average redundancy	20.6 (21.5)	11.7 (12.1)	5.0 (5.1)	20.8 (20.9)
% completeness	100.0 (100.0)	99.9 (100.0)	99.3 (99.1)	100.0 (100.0)
R_{merge}	0.204	0.173	0.134	0.235
$\langle I/\sigma(I)\rangle$	25.0 (2.88)	21.2 (2.03)	13.7 (2.07)	16.7 (1.94)

that it is displaced by a second plane formed by hydrated ions of opposite charge.[22] The behavior of the attachment of lysozyme molecules (positively charged molecules at the pH value of the buffer) to the cathode (a negatively charged electrode) could be explained based on the double layer effect. The double layer effect of two ITO electrodes dipped in the growth cell containing the protein solution, and the crystallizing agent may arise from the interaction of lysozyme with the ions present in the electric double layer around the electrode.

The polarity of ITO electrodes working as cathode (negatively charged) or anode (positively charged), in this electrolytic cell has been already represented in Figure 1. This experimental setup produces a migration of the positively charged lysozyme molecules (at pH 4.45) toward the cathode (−) or ferritin molecules (negatively charged at pH 5.52) toward the anode (+). Therefore, the surface of the cathode (−) of this growth cell will be initially filled with a plane of water molecules with their dipoles oriented with respect to the electrode charge and subsequently the positively charged macro-ions of the protein molecule itself (positively charged at this pH value) will be attached on it. This effect leads to a disturbance of the system owing to the fact that negatively charged ions (Cl^-) are needed for the protein−protein interactions in lysozyme crystallization.[23] This general overview explains why the crystals grew on the surface of the electrode when it was used as negatively charged electrode. For ferritin molecules (negatively charged at this pH value) the process is exactly the opposite. However, as has been already described by Moreno and Rivera,[8] Cd^{2+} ions are fixed on the initial water plane layer suffering a redox process forming a metal clusters and then the ferritin molecules are deposited on the surface of metallic cadmium. Then ferritin molecules are crystallized and grown by the ammonium sulfate used as precipitating agent.

This electrochemistry-based method of crystallizing proteins is not an electrocrystallization because there is no redox reaction occurring between the protein and the electrode, but there is an electro-focusing or electro-dialysis arising from the applied current. Something similar to this occurs in the classical electrophoresis method.

It was noticed for both proteins, lysozyme and ferritin, that crystals grown in electric field, were strongly attached to the cathode (negatively charged electrode), and to the anode (positively charged electrode) respectively. The crystal adhesion

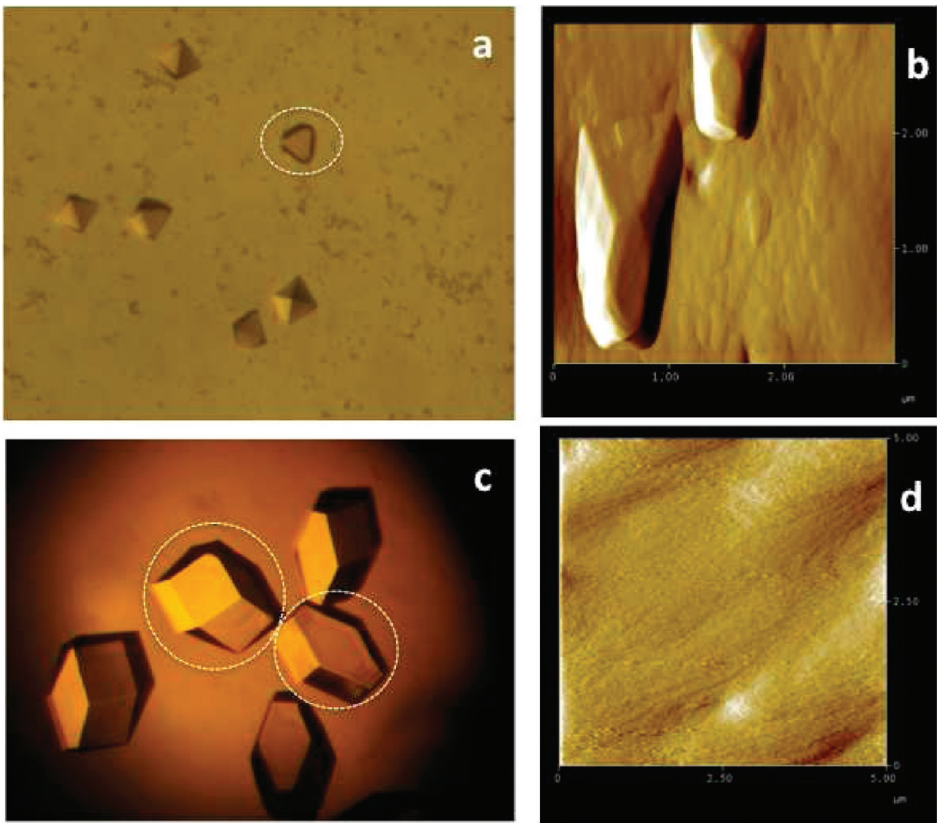

Figure 4. Crystals with specific faces perpendicularly oriented to the surface of the electrode attached to the ITO and useful for atomic force topography as shown in a white dotted circle for (a) ferritin, (b) 3.0 × 3.0 μm^2 AFM crystal surface image of ferritin, (c) lysozyme crystals, and (d) 5.0 × 5.0 μm^2 AFM crystal surface image of lysozyme.

was highly efficient, which made it easy to study the surface of these crystals with atomic force microscopy. The adhesion of protein crystals for research on crystal growth mechanisms, by means of atomic force microscopy (AFM), has been a handicap for AFM investigations for a long time, although there are few efforts about it already pusblished elsewhere suggesting different experimental designs for fixing 2D and 3D protein crystals.[24−29] All crystals for AFM scanning were perpendicularly orientated to the ITO electrode surface (Figure 4), which facilitate the scanning and proper contact with the tip and the cantilever. By using optical microscopy coupled to the AFM, it was possible to observe and locate the single crystal to be scanned. Since no changes on the structural characteristics of the crystal were observed, it was clear that the special crystal/precipitating solution system prevented the degradation of the single crystals and therefore the loss of structural information. Deflection of the tip was monitored by applying a small force (0.3 N/m) to the crystal. Since no movement was detected when pushing the crystal with the tip, while scanning, it is reasonable to assume that the crystal adhesion to the ITO electrode, due to the electric current applied during crystal growth, is strong enough to prevent the movement of the crystal during typical AFM scanning (as shown in the movie in the Supporting Information included). When scanning on the surface of ferritin crystals small hillock crystals (perhaps grown during the process) were observed and scanned (Figure 4b), while in lysozyme this type of satellite crystals were not observed (Figure 4d). The application of this novel crystal growth cell will control the surface deposition (on the cathode or on the anode) depending on the charge of the studied protein.

4. CONCLUSIONS

Nowadays, some physicochemical parameters, such as magnetic fields,[30] AC field,[31] low applied voltage,[32] nonphotochemical laser pulses for nucleation induction,[33] dynamic light scattering[34] are useful tools to separate both the nucleation and crystal growth process, which are usually connected processes. Mostly, these contributions have given us the tools to control the nucleation and, in some cases, to improve the protein crystal quality. In this contribution we have shown that different proteins need a specific current (ranging from 2 μA to 6 μA), between which the crystal quality is improved. The electrochemical adhesion of these crystals, imposed by the current and the conductivity of the ITO electrodes, depends also on the charge of the studied protein fixed by the working pH, and the isoelectric point value of the protein. Further more an important consideration is the size of the cell. The smaller the cell the smaller the value of current needed to avoid Indium Tin Oxide desorption. So, we need to be cautious when reproducing the experimental set up following the growth cell dimensions presented in this contribution.

Finally, we can conclude that the crystal growth cell presented in this contribution shows two practical applications: (1) for enhancing the protein crystal quality at very specific current values, and (2) in atomic force microscopy investigations as mean for fixing protein crystals. In future experiments comparative AFM experiments should be performed to study the effect of applied current on crystal quality by observing surface of crystals obtained in different experimental conditions.

■ ASSOCIATED CONTENT

Supporting Information. Video as described in the text. This material is available free of charge via the Internet at http://pubs.acs.org.

■ AUTHOR INFORMATION

Corresponding Author

*Address: Instituto de Quimica, Universidad Nacional Autonoma de Mexico, Circuito Exterior C.U. Mexico, D.F. 04510, Mexico. Phone: +52-55-56224467. Fax: +52-55-56162217. E-mail: carcamo@unam.mx.

■ ACKNOWLEDGMENT

The authors acknowledge the X-ray diffraction from the Laboratorio de Estructura de Proteinas-LANEM at UNAM (Mexico) and the help from M. Sci. Georgina E. Espinosa-Pérez. X-ray experiments were carried out at the X6A beamline at the National Synchrotron Light Source supported by the NIGMS and DOE under contract GM-0080 and DE-AC02-98CH10886. We acknowledge the professional grammar and style English revision done by Ms. Antonia Sánchez-Marín. We sincerely thank the help of Dr. Juan Pablo Reyes-Grajeda from the National Institute of the Genomic Medicine (INMEGEN) for processing high quality crystallographic images of Lysozyme crystals grown at different currents. One of the authors (R.R.R-A) acknowledges the PhD schoolarship from the Institute of Science and Technology of Mexico City (ICyTDF) as well as C.L.A.F., and schoolarship as research assistant from the SNI-CONACYT(Mexico). Finally one of the authors (A.M.) acknowledges the finantial support from DGAPA-UNAM Project PAPIIT No. IN201811-3.

■ REFERENCES

(1) Chin, C.; Dence, J. B.; Warren, J. C. *J. Biol. Chem.* **1976**, *251*, 3700–3705.
(2) Köhler, M.; Friedrich, J.; Fidy, J. *Biochim. Biophys. Acta* **1998**, *1386*, 255–288.
(3) Fidy, J.; Balog, E.; Köhler, M. *Biochim. Biophys. Acta* **1998**, *1386*, 289–303.
(4) Taleb, M.; Didierjean, C.; Jelsch, C.; Mangeot, J. P.; Capelle, B.; Aubry, A. *J. Cryst. Growth* **1999**, *200*, 575–582.
(5) Taleb, M.; Didierjean, C.; Jelsch, C.; Mangeot, J. P.; Aubry, A. *J. Cryst. Growth* **2001**, *232*, 250–255.
(6) Nanev, C.; Penkova, A. *J. Cryst. Growth* **2001**, *232*, 285–293.
(7) Mirkin, N.; Frontana-Uribe, B. A.; Rodríguez-Romero, A.; Hernández-Santoyo, A.; Moreno, A. *Acta Crystallogr., Sect. D: Biol. Crystallogr.* **2003**, *59*, 1533–1538.
(8) Moreno, A.; Rivera, M. *Acta Crystallogr., Sect. D: Biol. Crystallogr.* **2005**, *61*, 1678–1681.
(9) Al-Haq, M. I.; Lebrasseur, E.; Tsuchiya, H.; Torii, T. *Crystallogr. Rev.* **2007**, *13*, 29–64.
(10) Frontana-Uribe, B. A.; Moreno, A. *Cryst. Growth Des.* **2008**, *8*, 4194–4199.
(11) Zoubida, H.; Veesler, S. *Prog. Biophys. Mol. Biol.* **2009**, *101*, 38–44.
(12) Bolanos-Garcia, V. M.; Chayen, N. *Prog. Biophys. Mol. Biol.* **2009**, *101*, 3–12.
(13) Hammadi, Z.; Astier, J. P.; Morin, R.; Veesler, S. *Cryst. Growth Des.* **2007**, *7*, 1472–1475.
(14) Koizumi, H.; Fujiwara, K.; Uda, S. *Cryst. Growth Des.* **2009**, *9*, 2420–2424.
(15) Sazaki, G.; Moreno, A.; Nakajima, K. *J. Cryst. Growth* **2004**, *262*, 499–502.
(16) Surade, S.; Ochi, T.; Nietlispach, D.; Chirgadze, D.; Moreno, A. *Cryst. Growth Des.* **2010**, *10*, 691–699.
(17) Gavira, J. A.; García-Ruiz, J. M. *Cryst. Growth Des.* **2009**, *9*, 2610–2615.
(18) Yin, D. C.; Geng, L. Q.; Lu, Q. Q.; Lu, H. M.; Shang, P.; Wakayama, N. I. *Cryst. Growth Des.* **2009**, *9*, 5083–5091.
(19) Maki, S.; Ishikawa, K.; Ataka, M. *J. Cryst. Growth* **2009**, *311*, 4725–4729.
(20) Kimura, F.; Mizutani, K.; Mikami, B.; Kimura, T. *Cryst. Growth Des.* **2011**, *11*, 12–15.
(21) Otwinowski, Z.; Minor, W. *Methods in Enzymology: Macromolecular Crystallography*; Carter, C. W., Jr., Sweet, R. M., Eds.; Academic Press: New York, 1997; Vol. 276, part A, pp 307−326.
(22) Crow, D. R. In *Principles and Applications of Electrochemistry*; Chapman and Hall, Ltd.: London, 1979; Chapter 7, pp 150−151.
(23) Vaney, M. C.; Broutin, I.; Retailleau, P.; Douangamath, A.; Lafont, S.; Hamiaux, C.; Prangé, T.; Ducruix, A.; Riés-Kautt, M. *Acta Crystallogr., Sect. D: Biol. Crystallogr.* **2001**, *57*, 929–940.
(24) Dorn, I. T.; Hofmann, U. G.; Peltonen, J.; Tampé, R. *Langmuir* **1998**, *14*, 4836–4842.
(25) Yamamoto, D.; Nagura, N.; Omote, S.; Taniguchi, M.; Ando, T. *Biophys. J.* **2009**, *97*, 2358–2367.
(26) El-Kirat, K.; Burton, I.; Dufrene, Y. F. *J. Microsc.* **2005**, *218*, 199–207.
(27) Ko, T. P.; Kuznetsov, Y. G.; Malkin, A. J.; Day, J.; McPherson, A. *Acta Crystallogr., Sect. D: Biol. Crystallogr.* **2001**, *57*, 829–839.
(28) Hernández-Pérez, T.; Mirkin, N.; Moreno, A.; Rivera, M. *Electrochem. Solid State Lett.* **2002**, *5*, 37–39.
(29) Acosta, F.; Eid, D.; Marín-García, L.; Frontana-Uribe, B. A.; Moreno, A. *Cryst. Growth Des.* **2007**, *7*, 2187–2191.
(30) Sazaki, G. *Prog. Biophys. Mol. Biol.* **2009**, *101*, 45–55.
(31) Hou, D.; Chang, H. C. *App. Phys. Lett.* **2008**, *92*, 223902.
(32) Wakamatsu, T.; Ohnishi, Y. *Jpn. J. Appl. Phys.* **2011**, *50*, 048003-1–048003-2.
(33) Lee, I. S.; Evans, J. M. B.; Erdemir, D.; Lee, A. Y.; Garetz, B. A.; Myerson, A. S. *Cryst. Growth Des.* **2008**, *8*, 4255–4261.
(34) Saridakis, E.; Dierks, K.; Moreno, A.; Dieckmann, M. W. M.; Chayen, N. *Acta Crystallogr., Sect. D: Biol. Crystallogr.* **2002**, *58*, 1597–1600.